
MACHINE LEARNING BASED DIMENSION REDUCTION FOR A STABLE MODELING OF PERIODIC FLOW PHENOMENA

Hiroshi Omichi

Department of Mechanical Engineering, Keio University;
Department of Mechanical and Aerospace Engineering, University of California, Los Angeles
hiroshi.omichi@keio.jp

Takeru Ishize

Department of Mechanical Engineering, Keio University
takeru.ishize@keio.jp

Koji Fukagata

Department of Mechanical Engineering, Keio University
fukagata@mech.keio.ac.jp

November 16, 2023

ABSTRACT

In designing efficient feedback control laws for fluid flow, the modern control theory can serve as a powerful tool if the model can be represented by a linear ordinary differential equation (ODE). However, it is generally difficult to find such a linear model for strongly nonlinear and high-dimensional fluid flow phenomena. In this study, we propose an autoencoder which maps the periodic flow phenomena into a latent dynamics governed by a linear ODE, referred to as a pseudo-symplectic Linear system Extracting AutoEncoder (LEAE). In addition to the normal functionality of autoencoder, pseudo-symplectic LEAE emulates a symplectic time integration scheme so that the Hamiltonian (*i.e.*, the pseudo-energy) of the latent variables is conserved. We demonstrate that the stability of the derived ODE is improved by considering the integration stepping forward and backward at the same time. Here, we consider the circular cylinder wake at $Re_D = 100$ as a typical periodic flow phenomenon.

Keywords Autoencoder · Linear system extraction · Reduced order modeling · Pseudo-symplectic

1 Introduction

Particularly when a target state of flow control locates far away from its base state, active flow control (Park *et al.*, 1994; Naito and Fukagata, 2014; Jin *et al.*, 2020) is one of the promising techniques in terms of its efficacy and degrees of freedom in its design. Among the active control strategies, model-free approaches (Rabault *et al.*, 2019; Wang *et al.*, 2023) have strong merits in their capability to follow the shifted dynamics and its transient process, although it is difficult to interpret or generalize the constructed controllers (Brunton and Noack, 2015). Model-based approaches have strong advantages also in that the existing control theories can be applied; when the model can be represented by a linear ODE, there is a wide range of options like linear quadratic regulator even though they are only valid as long as the controlled states can be linearly approximated around the model. However, as can easily be imagined, it is difficult to find a proper model which governs fluid flow phenomena due to their high-dimensionality and strong nonlinearity. In this context, dimension reduction with machine learning and modeling for the temporal evolution of low-dimensionalized variables (*i.e.*, latent variables) have been investigated (Milano and Koumoutsakos, 2002; Brenner

et al., 2019; Hasegawa *et al.*, 2020; Brunton *et al.*, 2020a; Farazmand and Saibaba, 2023); however, with a naïve dimension reduction, the extracted latent dynamics will remain highly nonlinear (Fukami *et al.*, 2021).

To address this problem, we propose an enhanced autoencoder named pseudo-symplectic Linear system Extracting AutoEncoder (LEAE) to compress flow field data into a latent space such that the latent dynamics is governed by a linear ODE. Inside the pseudo-symplectic LEAE, the dimension reduction is performed with an autoencoder, assuming the time integration of latent variables using the Crank-Nicolson scheme. In particular, we propose a method accounting for the symplectic property of the latent system by training the temporal evolution in forward and backward directions simultaneously. By so doing, the Hamiltonian (*i.e.*, the pseudo-energy) of the latent variables $H = \frac{1}{2} \sum_i \varphi_i^2$ is conserved, where φ_i denotes i -th component of the latent vector φ .

In this study, we consider the iconic periodic flow phenomena in this field, *i.e.*, the periodic circular cylinder wake at the Reynolds number $Re_D = 100$.

2 Methods

2.1 Dataset

To prepare the training data, let us consider the two-dimensional flow around a circular cylinder at the Reynolds number based on its diameter $Re_D = 100$. We use direct numerical simulation (DNS) (Kor *et al.*, 2017), and the governing equations are the continuity and Navier-Stokes equations for incompressible flows,

$$\nabla \cdot \mathbf{u} = 0, \quad (1)$$

$$\frac{\partial \mathbf{u}}{\partial t} + \nabla \cdot (\mathbf{u}\mathbf{u}) = -\nabla p + \frac{1}{Re_D} \nabla^2 \mathbf{u}, \quad (2)$$

where $\mathbf{u} = \{u, v\}$ and p are the velocity vector and pressure, respectively. Both quantities are nondimensionalized by the fluid density ρ^* , the diameter of cylinder D^* , and the uniform velocity U_∞^* , where $(\cdot)^*$ denotes dimensional quantities.

The left side of Figure 1 indicates the computational domain with the streamwise (x) and transverse (y) lengths of $25.6D$ and $20.0D$, respectively. A uniform inflow velocity of $U_\infty = 1$, free-slip conditions on the upper and lower boundaries, and a convective boundary condition on the outflow boundary are applied, while the ghost-cell method (Kor *et al.*, 2017) is utilized to impose the no-slip boundary condition on the surface. A uniform Cartesian grid system is used, and the number of grid points in each direction is $(N_x, N_y) = (1024, 800)$, and the center of the cylinder locates at $x = 9D$ downstream from the inflow boundary in x direction and at the center in y direction. The time step is $\Delta t_{\text{DNS}} = 2.5 \times 10^{-3}$.

For training of a machine learning model, the velocity fields (u, v) inside the confined region depicted with the blue line in Figure 1 is used to extract the key feature of the cylinder wake. The size of a snapshot is $(384 \times 192 \times 2)$, and we use the developed wake shedding of 2000 snapshots with a time step of $\Delta t_{\text{Data}} = 2.5 \times 10^{-2}$ as the dataset for the machine learning model.

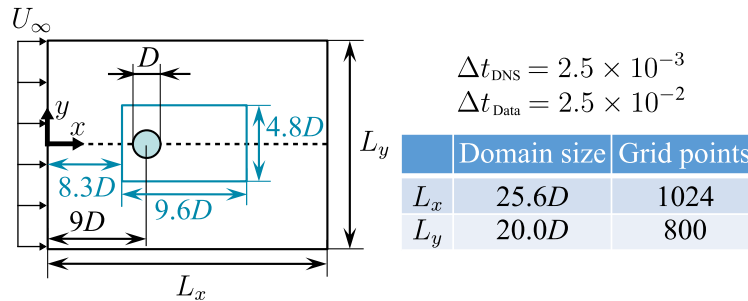


Figure 1: Computational configuration of DNS.

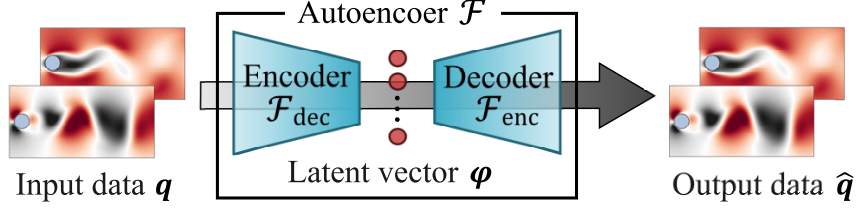


Figure 2: Schematic of a typical autoencoder.

2.2 Pseudo-symplectic linear system extraction autoencoder

2.2.1 Autoencoder

The machine learning model of this study is based on the concept of autoencoder (Hinton and Salakhutdinov, 2006) to reduce the dimension of data. In what follows, general description of autoencoders is detailed. As illustrated in Figure 2, an autoencoder \mathcal{F} is comprised of an encoder \mathcal{F}_{enc} and a decoder \mathcal{F}_{dec} with a bottleneck in the middle. As long as the autoencoder precisely replicates the input data $\mathbf{q} \in \mathbb{R}^{n_H}$ and output it as $\hat{\mathbf{q}} \in \mathbb{R}^{n_H}$, it can be said that the encoder maps the high dimensional data into its low dimensional representation $\boldsymbol{\varphi} \in \mathbb{R}^{n_L}$, *i.e.*, latent variables (vector), and the decoder has the inverse function. Note that n_H and n_L denote the dimension of the original and the low-dimensionalized data (usually, $n_H \gg n_L$), and the latent variables $\boldsymbol{\varphi}$ probably hold essential characteristics of the original dynamics of \mathbf{q} . This conversion can be formulated as

$$\mathbf{q} \approx \hat{\mathbf{q}} = \mathcal{F}(\mathbf{q}; \mathbf{w}) = \mathcal{F}_{\text{dec}}(\boldsymbol{\varphi}) = \mathcal{F}_{\text{dec}}(\mathcal{F}_{\text{enc}}(\mathbf{q})), \quad (3)$$

where \mathbf{w} denotes the weights inside the machine learning model to be optimized so that

$$\mathbf{w} = \operatorname{argmin}_{\mathbf{w}} \|\mathbf{q} - \hat{\mathbf{q}}\|_2. \quad (4)$$

In terms of the network architecture, we follow Hasegawa *et al.* (2020) and employ nonlinear neural networks, *i.e.*, Convolutional Neural Network (LeCun *et al.*, 1998) (CNN) and Multi-layer perception (Rumelhart *et al.*, 1986).

2.2.2 Linear ODE layer

After the dimension reduction, the temporal evolution of the latent variables have to be modeled to construct a reduced order model. In this study, the temporal evolution is predicted with what we call the linear ODE (LODE) layer, which follows a temporal discretization of linear ODEs using the Crank-Nicolson scheme. Considering a linear ODE,

$$\dot{\boldsymbol{\varphi}} = \mathbf{A}\boldsymbol{\varphi}, \quad (5)$$

where $\boldsymbol{\varphi} \in \mathbb{R}^{n_L}$ corresponds to the latent vector in section 2.2.1, and \mathbf{A} is the coefficient matrix to be optimized through the training process, equation (5) can be discretized with Crank-Nicolson scheme as

$$\frac{\boldsymbol{\varphi}(t + \Delta t) - \boldsymbol{\varphi}(t)}{\Delta t} = \frac{\mathbf{A}[\boldsymbol{\varphi}(t + \Delta t) + \boldsymbol{\varphi}(t)]}{2} \quad (6)$$

$$\Rightarrow \boldsymbol{\varphi}(t + \Delta t) = (2\mathbf{I} + \Delta t\mathbf{A})(2\mathbf{I} - \Delta t\mathbf{A})^{-1}\boldsymbol{\varphi}(t). \quad (7)$$

Regarding $\boldsymbol{\varphi}(t)$ and $\boldsymbol{\varphi}(t + \Delta t)$ as input and output, respectively, we can use a single MLP layer corresponding to $n_L \times n_L$ matrix \mathbf{A} .

2.2.3 Overview of pseudo-symplectic linear system extraction autoencoder

Here, the overview of our machine learning model, pseudo-symplectic linear system extraction autoencoder (LEAE), is summarized in Figure 3. The pseudo-symplectic LEAE basically consists of the encoder, the decoder, and the LODE layer in the middle. Both of the encoders completely share the weights, and both of the decoders do as well, which means that only a single encoder and decoder are trained here. Needless to say, the encoder and the decoder are trained to duplicate the original snapshot as precisely as possible, but what we want to highlight here is the usage of snapshots mainly to train LODE layer. LODE layer is trained to not only predict $\boldsymbol{\varphi}(t + \Delta t)$ from $\boldsymbol{\varphi}(t)$ (the orange arrows) but also $\boldsymbol{\varphi}(t)$ from $\boldsymbol{\varphi}(t + \Delta t)$ (the purple arrows). By doing so, LODE layer can be trained so as to satisfy the time reversal symmetry, which is the important property of symplectic integrators that must be satisfied in the time

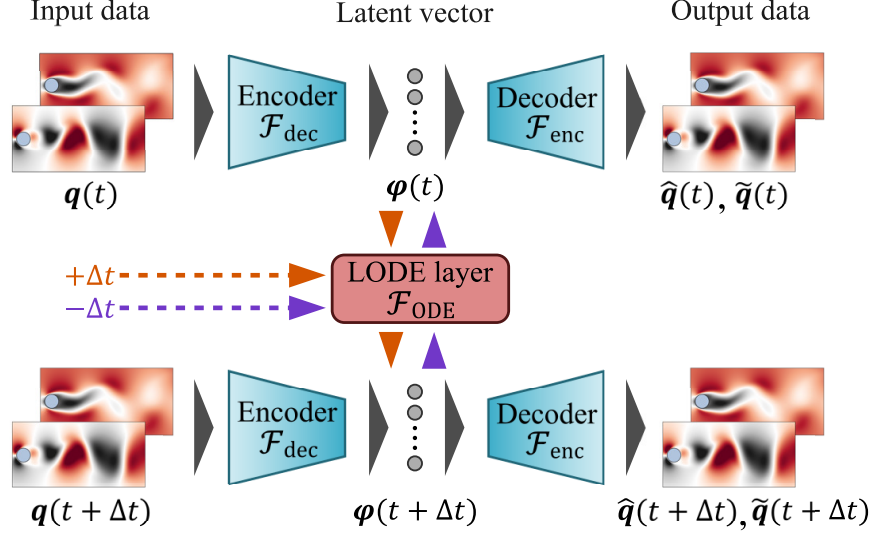


Figure 3: Schematic of pseudo-symplectic linear system extraction autoencoder.

integration of Hamiltonian system (Aceto and Trigiante, 1999). In sum, the present training process consists of four types of operations:

$$\begin{cases} \hat{q}(t) &= \mathcal{F}_{\text{dec}}(\mathcal{F}_{\text{enc}}(q(t))) = \mathcal{F}_{\text{dec}}(\varphi(t)) \\ \hat{q}(t + \Delta t) &= \mathcal{F}_{\text{dec}}(\mathcal{F}_{\text{enc}}(q(t + \Delta t))) = \mathcal{F}_{\text{dec}}(\varphi(t + \Delta t)) \\ \tilde{q}(t + \Delta t) &= \mathcal{F}_{\text{dec}}(\mathcal{F}_{\text{ODE}}(\varphi(t), \Delta t)) \\ \tilde{q}(t) &= \mathcal{F}_{\text{dec}}(\mathcal{F}_{\text{ODE}}(\varphi(t + \Delta t), -\Delta t)) \end{cases}, \quad (8)$$

where Δt is a time step. While the former two equations contribute to guaranteeing that \mathcal{F}_{enc} and \mathcal{F}_{dec} are providing the nonlinear mappings at exactly the same time indices, the latter two commit to learning the temporal evolution stepping forward and backward, and all operations are taken simultaneously. Therefore, the loss function is defined as

$$\mathcal{L} = \| q(t) - \hat{q}(t) \|_2 + \| q(t + \Delta t) - \hat{q}(t + \Delta t) \|_2 + \| q(t + \Delta t) - \tilde{q}(t + \Delta t) \|_2 + \| q(t) - \tilde{q}(t) \|_2. \quad (9)$$

3 Results

In this section, the efficacy of the pseudo-symplectic manner is summarized by comparing the pseudo-symplectic LEAE and a naïve LEAE. Here, the naïve LEAE is a form of LEAE which excludes the temporally inverse procedure denoted as the purple arrows in figure 3.

Figure 4 visualizes the performances of the naïve LEAE (blue plots) and the pseudo-symplectic LEAE (red plots). In figure 4 (a) and (b), the latent variables encoded from flow fields (gray lines) and ones predicted with numerical integration of the derived ODEs (colored lines) are compared. While the predicted trajectories blow up in the case of the naïve LEAE, the encoded flow fields and the result of numerical integration show a nice agreement in the case of the pseudo-symplectic LEAE. Note that the initial values for the cases of the numerical integration are given through encoding the initial flow fields. In figure 4 (c) and (d), both types of LEAEs are evaluated in terms of L_2 error of decoded fields at each snapshot, and means and standard deviations taken over three-fold cross validation are presented. Shown in figure 4 (c) is the errors of the reconstructed flow fields through the autoencoder. Please note that no temporal evolution is considered here; the reconstruction procedure corresponds to the horizontal flow in figure 3, and the error is exactly the same as the first term of the equation (9). The errors including those along the temporal evolution are presented in figure 4 (d). Here, decoded fields from the predicted trajectories in figure 4 (a) and (b) are assessed. The above two evaluations demonstrate that the pseudo-symplectic LEAE is a substantially improved method compared to the naïve one.

4 Conclusions

In this study, we proposed a pseudo-symplectic Linear system Extraction AutoEncoder (LEAE) to extract a low-dimensionalized dynamics which is governed by a linear ODE. It has been shown that the pseudo-symplectic LEAE has

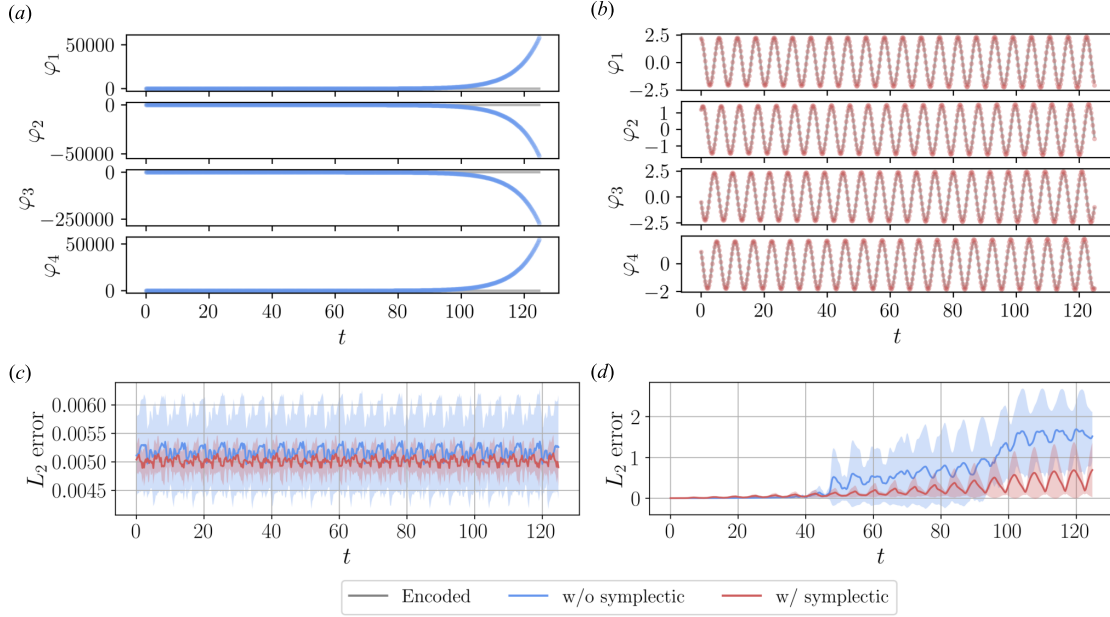


Figure 4: The performances of the naive LEAE (blue plots) and the pseudo-symplectic LEAE (red plots). (a), (b) reproduced latent trajectories, (c) L_2 error of reconstructed fields, and (d) L_2 error of decoded fields from the reproduced latent trajectories.

the ability to derive an ODE which models a periodic latent dynamics more precisely than a naïve LEAE. However, in the present study, we only considered the case where the ODE strongly adheres to a limit-cycle corresponding to the periodic wake shedding, and this modeling is imaginably not applicable for cases where flow states are shifting. Toward an effective flow control framework, there is room for further research into a modeling capable of following transient processes due to control inputs.

Acknowledgments

This work was supported by JSPS KAKENHI Grant Number 21H05007. The authors acknowledge Mr. Shoei Kanehira (Keio University) for fruitful discussion and comments.

References

- Aceto, L. and Trigiante, D. (1999), “Symmetric schemes, time reversal symmetry and conservative methods for Hamiltonian systems,” *Journal of Computational and Applied Mathematics*, Vol. 107. pp. 257–274.
- Brenner, M.P., Eldredge, J.D. and Freund, J.B. (2019), “Perspective on machine learning for advancing fluid mechanics,” *Physical Review Fluids*, Vol. 4, Article No. 100501.
- Brunton, S.L. and Noack, B.R. (2015), “Closed-loop turbulence control: Progress and challenges,” *Applied Mechanics Reviews*, Vol. 67, Article No. 050801.
- Brunton, S.L., Hemati, M.S. and Taira, K. (2020a), “Special issue on machine learning and data-driven methods in fluid dynamics,” *Theoretical and Computational Fluid Dynamics*, Vol. 34, pp. 333–337.
- Farazmand M. and Saibaba, A.K. (2023), “Tensor-based flow reconstruction from optimally located sensor measurements,” *Journal of Fluid Mechanics*, Vol. 962, Article No. A27.
- Fukami, K., Murata, T., Zhang, K., and Fukagata, K. (2023), “Sparse identification of nonlinear dynamics with low-dimensionalized flow representations,” *Journal of Fluid Mechanics*, Vol. 926, Article No. A10.
- Hasegawa, K., Fukami, K., Murata, T. and Fukagata, K. (2020), “Machine-learning-based reduced-order modeling for unsteady flows around bluff bodies of various shapes,” *Theoretical and Computational Fluid Dynamics*, Vol. 34, pp. 367–383.

- Hinton, G.E. and Salakhutdinov, R.R. (2006), “Reducing the dimensionality of data with neural networks,” *Science*, Vol. 313, pp. 504–507.
- Jin, B., Illingworth, S. J., and Sandberg, R. D. (2020), “Feedback control of vortex shedding using a resolvent-based modelling approach,” *Journal of Fluid Mechanics*, Vol. 897, Article No. A26.
- Kor, H., Badri Ghomizad, M. and Fukagata, K. (2017), “A unified interpolation stencil for ghost-cell immersed boundary method for flow around complex geometries,” *Journal of Fluid Science and Technology*, Vol. 12, Article No. JFST0011.
- LeCun, Y., Bottou, L., Bengio, Y. and Haffner, P. (1998), “Gradient-based learning applied to document recognition”, *Proceedings of the IEEE*, Vol. 86, pp. 2278–2324.
- Milano, M. and Koumoutsakos, P. (2002), “Neural network modeling for near wall turbulent flow”, *Journal of Computational Physics*, Vol. 182, pp. 1–26.
- Naito, H. and Fukagata, K. (2014), “Control of flow around a circular cylinder for minimizing energy dissipation”, *Physical Review E*, Vol. 90, Article No. 053008.
- Park, D.S., Ladd, D.M. and Hendricks, E.W. (1994), “Feedback control of von Kármán vortex shedding behind a circular cylinder at low Reynolds numbers”, *Physics of Fluids*, Vol. 6, pp. 2390–2405.
- Rabault, J., Kuchta, M., Jensen, A., Réglade, U. and Cerardi, N. (2019), “Artificial neural networks trained through deep reinforcement learning discover control strategies for active flow control”, *Journal of Fluid Mechanics*, Vol. 865, pp. 281–302.
- Rumelhart, D.E., Hinton, G.E. and Williams, R.J. (1986), “Learning representations by back-propagating errors”, *Nature*, Vol. 323, pp. 533–536.
- Wang, Z., Fan, D., Jiang, X., Triantafyllou, M. S., and Karniadakis, G. E. (2023), “Deep reinforcement transfer learning of active control for bluff body flows at high Reynolds number”, *Journal of Fluid Mechanics*, Vol. 973, Article No. A32.